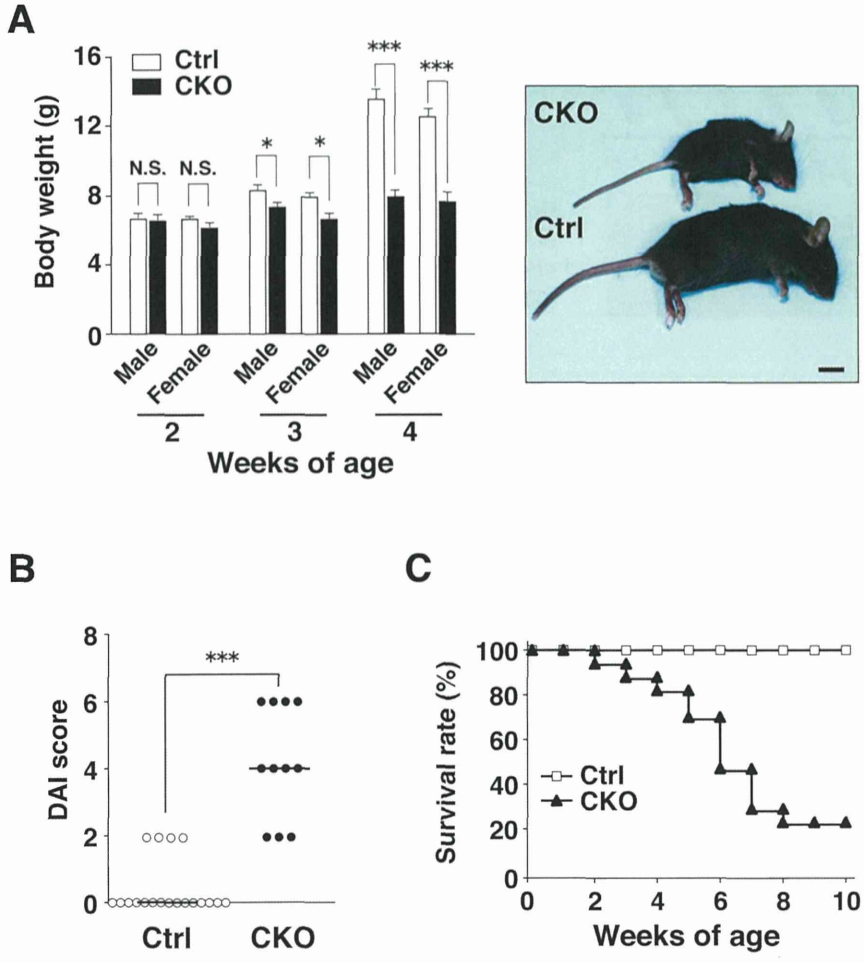

Figure 2. Shp2 CKO mice develop severe colitis. A: Body weight of 2-, 3-, or 4-week-old control (male, $n=23$, 26, and 27, respectively; female, $n=22$, 24, and 22, respectively) or Shp2 CKO (male, $n=17$, 20, and 16, respectively; female, $n=15$, 15, and 13, respectively) mice is shown in the left panel. Data are means ± SE. *$P<0.05$, ***$P<0.0001$ (Welch's t test). N.S., not significant. Representative photographs of control and Shp2 CKO mice at 5 weeks of age are shown in the right panel. Scale bar, 1 cm. **B**: Disease activity index (DAI) for colitis in control ($n=19$) and Shp2 CKO ($n=11$) mice at 4 to 5 weeks of age. Bars indicate median scores. ***$P<0.0001$ (Wilcoxon rank-sum test). **C**: Survival rates of control ($n=19$) and Shp2 CKO ($n=17$) mice.
doi:10.1371/journal.pone.0092904.g002

base to the farthest migrated BrdU-positive cells and was measured with the use of ImageJ software (NIH).

Intestinal organoid culture

Intestinal organoid culture was performed as previously described [5]. In brief, crypts were isolated from the small intestine by incubation for 30 min in PBS containing 2 mM EDTA. The isolated crypts were mixed with Matrigel (BD Biosciences) and transferred to 48-well plates. After polymerization of the Matrigel, advanced Dulbecco's modified Eagle's medium–F12 (Invitrogen), which was supplemented with penicillin-streptomycin (100 U/ml) (Invitrogen), 10 mM HEPES (Invitrogen), 1× GlutaMAX (Invitrogen), 1× N2 (Invitrogen), 1× B27 (Invitrogen), 1.25 mM *N*-acetylcysteine (Sigma-Aldrich), epidermal growth factor (500 ng/ml) (Peprotech, Rocky Hill, NJ), 10% R-spondin1–Fc–conditioned medium, and Noggin (100 ng/ml) (Peprotech), was overlaid on the gel in each well. The cultures were then maintained in an incubator (37°C, 5% CO_2). Images were obtained with a microscope (Axiovert 200; Carl Zeiss, Oberkochen, Germany).

Statistical analysis

Disease activity was compared between mouse genotypes with the Wilcoxon rank-sum test. Other quantitative data are presented as means ± SE and were analyzed with Student's t test, the Wilcoxon rank-sum test, or Welch's t test as appropriate. All statistical analysis was performed with JMP software version 9.0 (SAS Institute, Cary, NC). A P value of <0.05 was considered statistically significant.

Results

Generation of IEC-specific Shp2 CKO mice

To examine the impact of Shp2 ablation in IECs, we crossed mice homozygous for a floxed *Ptpn11* allele [15] with those harboring a transgene for Cre recombinase under the control of the villin gene promoter (villin-*cre*) [18]. The specificity and efficiency of *Ptpn11* deletion in adult *Ptpn11*$^{fl/fl}$;villin-*cre* (Shp2 CKO) mice were determined by PCR analysis of genomic DNA isolated from the intestine as well as from other organs. Consistent with the results of previous studies with the villin-*cre* transgene [18], deleted *Ptpn11* alleles were detected in the colon, ileum,

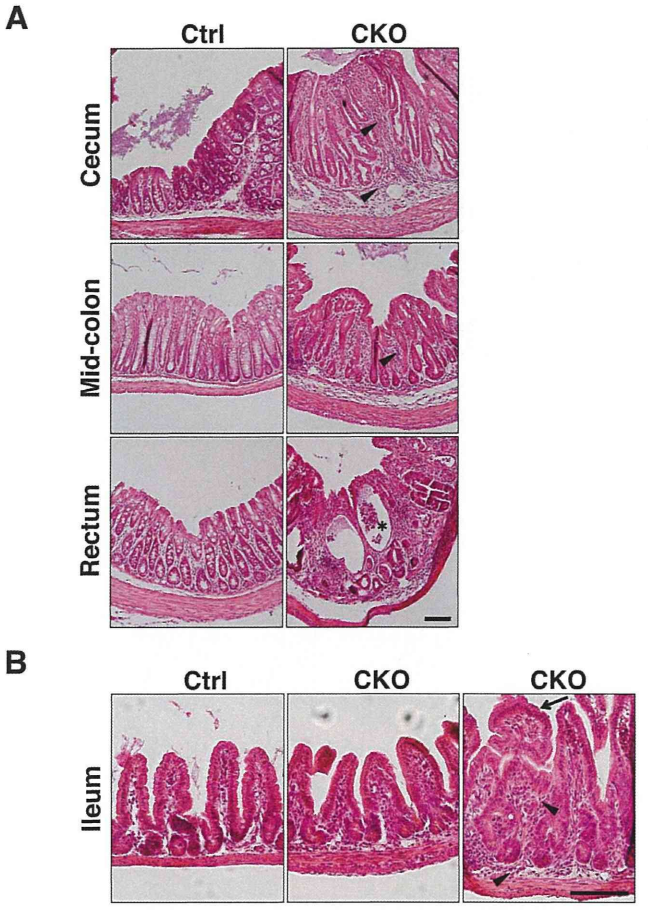

Figure 3. Spontaneous development of marked inflammation in the colon of Shp2 CKO mice. A: Hematoxylin-eosin staining of paraffin-embedded sections of the cecum, mid-colon, and rectum from control or Shp2 CKO mice at 3 weeks of age. Arrowheads and the asterisk indicate inflammatory infiltrates and a crypt abscess, respectively. **B**: Hematoxylin-eosin staining of the ileum from control and Shp2 CKO mice at 3 weeks of age. Arrowheads and the arrow indicate inflammatory infiltrates and abnormal villus structure, respectively. All data are representative of three separate experiments. Scale bars, 100 μm.
doi:10.1371/journal.pone.0092904.g003

jejunum, and duodenum of Shp2 CKO mice, but not in any other organ (**Fig. 1A**). We also confirmed that the activity of β-galactosidase was detected specifically in the entire epithelium of the ileum and colon of *R26R*;villin-*cre* mice (**Fig. S1**). Immunoblot analysis also showed that the abundance of Shp2 protein in isolated IECs from the ileum or colon of Shp2 CKO mice was greatly reduced compared with that for control mice, whereas it was unaffected in other organs (**Fig. 1B**). These results thus indicated that the villin-*cre* transgene directs the efficient and specific deletion of the Shp2 gene in IECs.

Shp2 CKO mice develop severe colitis

Shp2 CKO mice were born apparently healthy (data not shown), and they were phenotypically indistinguishable from control littermates at 2 weeks of age (**Fig. 2A**). However, both male and female Shp2 CKO mice manifested a marked reduction in body weight as well as growth retardation compared with control littermates at 3 to 4 weeks of age (**Fig. 2A**). They also manifested severe diarrhea. We evaluated disease activity for colitis on the basis of stool consistency, blood in the stool, and anorectal prolapse in both Shp2 CKO and control mice at 4 to 5 weeks of age. The disease activity index for Shp2 CKO mice was markedly greater than that for control animals (**Fig. 2B**). Furthermore, ~80% of Shp2 CKO mice died by 10 weeks of age (**Fig. 2C**).

Histological examination of the colon from 3-week-old Shp2 CKO mice revealed pronounced inflammation in all regions from the cecum to the rectum (**Fig. 3A**). Epithelial hyperplasia was relatively prominent, and transmural inflammation with crypt abscesses was occasionally observed. Inflammatory infiltrates were also present in both the mucosa and submucosa. In contrast to the colon, most regions of the small intestine of Shp2 CKO mice were phenotypically indistinguishable from those of control mice, although abnormal structures of villi and mild inflammatory infiltrates were occasionally apparent. Together, these observations indicated that Shp2 ablation in IECs resulted in the spontaneous development of marked inflammation in the intestine, particularly in the colon.

Marked reduction in the numbers of absorptive enterocytes and goblet cells in Shp2 CKO mice

We next examined the impact of IEC-specific Shp2 ablation on the numbers of absorptive enterocytes, mucin-secreting goblet cells, and antimicrobial peptide–producing Paneth cells in the intestinal epithelium. The number of absorptive enterocytes, which were identified on the basis of their morphology in tissue sections stained with a mAb to β-catenin [8], was markedly reduced in the ileum of Shp2 CKO mice at 3 to 4 weeks of age compared with that for control mice (**Fig. 4A**). We were not able to determine the precise number of absorptive enterocytes in the colon of Shp2 CKO mice because of their severe colitis. In addition, the number of mucin 2–positive goblet cells was also reduced in the ileum as well as the colon of Shp2 CKO mice at 3 weeks of age (**Fig. 4B**). We were again unable to determine the precise number of goblet cells in the colon of Shp2 CKO mice as a result of their severe colitis. In contrast, the number of lysozyme-positive Paneth cells was slightly increased in the ileum of Shp2 CKO mice at 3 weeks of age (**Fig. 4C**). These results thus suggested that Shp2 is important for regulation of the numbers of absorptive enterocytes and goblet cells in the mouse intestine.

We next investigated whether Shp2 regulates the size of the intestinal stem cell population, for which Olfm4 is a marker [24]. However, the number of Olfm4 mRNA–positive cells in crypts of the ileum did not differ between Shp2 CKO and control mice at 3 to 4 weeks of age (**Fig. 4D**).

Impaired migration of IECs in the ileum of Shp2 CKO mice

Given the role of Shp2 in promotion of cell growth or survival [10], we next examined the incorporation of BrdU into IECs as well as the turnover of BrdU-labeled IECs in Shp2 CKO mice at 3 to 4 weeks of age. At 2 h after BrdU injection, the number of BrdU-positive IECs in crypts of the ileum (**Fig. 5A**) or colon (**Fig. 5B**) from Shp2 CKO mice was similar to that for control mice. At 2 days after BrdU injection, most BrdU-positive IECs in the ileum of control mice had reached the middle region or top of villi (**Fig. 5C**). In contrast, such migration of BrdU-positive IECs along the crypt-villus axis was markedly delayed in Shp2 CKO mice (**Fig. 5C**). These results thus suggested that Shp2 is dispensable for the proliferation of IECs, in particular for that of TA cells, in crypts of the ileum or colon, but that it is required for migration of IECs along the crypt-villus axis in the ileum.

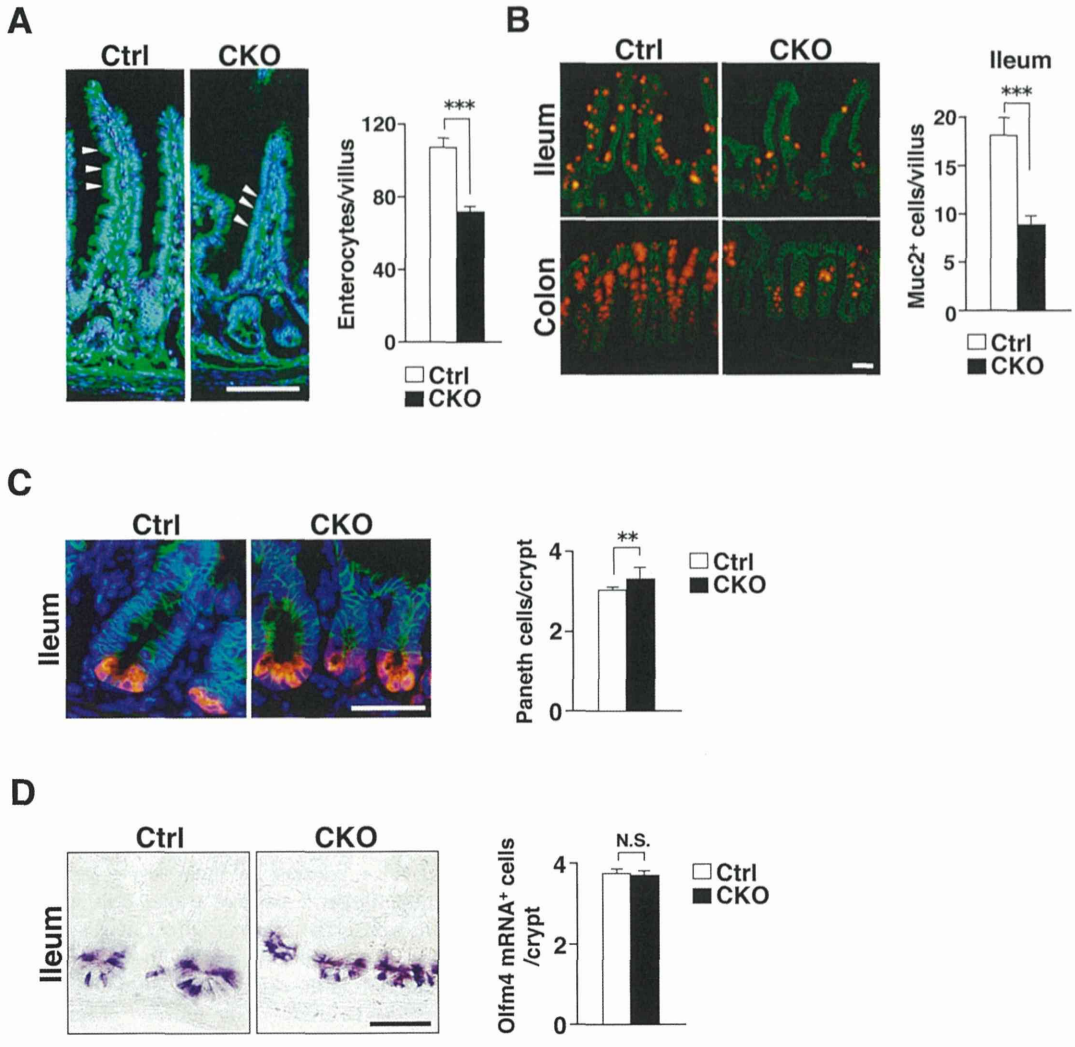

Figure 4. Marked reduction in the numbers of absorptive enterocytes and goblet cells in Shp2 CKO mice. A: Frozen sections of the ileum from control or Shp2 CKO mice at 3 to 4 weeks of age were immunostained with an antibody to β-catenin (green) and also stained with DAPI (blue). Representative images are shown in the left panel. Arrowheads indicate β-catenin–positive absorptive enterocytes. Scale bar, 100 μm. The number of β-catenin–positive absorptive enterocytes per villus was determined for the ileum (right panel). Data are means ± SE for 38 (control) or 32 (Shp2 CKO) villi from a total of three mice per group. ***$P<0.0001$ (Welch's t test). **B**: Frozen sections of the ileum and colon from control or Shp2 CKO mice at 3 weeks of age were immunostained with antibodies to mucin 2 (red) and to β-catenin (green). Representative images are shown in the left panel. Scale bar, 100 μm. The number of mucin 2 (Muc2)–positive goblet cells per villus was determined for the ileum (right panel). Data are means ± SE for 100 (control) or 93 (Shp2 CKO) villi from a total of three mice per group. ***$P<0.0001$ (Welch's t test). **C**: Frozen sections of the ileum from control or Shp2 CKO mice at 3 weeks of age were subjected to immunostaining with antibodies to lysozyme (red) and to β-catenin (green) as well as to staining of nuclei with DAPI (blue). Representative images are shown in the left panel. Scale bar, 50 μm. The number of lysozyme-positive Paneth cells per crypt was determined (right panel). Data are means ± SE for 150 crypts from a total of three mice per group. **$P<0.01$ (Student's t test). **D**: Paraffin sections of the ileum from control or Shp2 CKO mice at 3 to 4 weeks of age were subjected to in situ hybridization analysis of Olfm4 mRNA. Representative images are shown in the left panel. Scale bar, 50 μm. The number of Olfm4 mRNA–positive cells per crypt was determined (right panel). Data are means ± SE for 60 crypts from a total of two mice per group. N.S., not significant (Student's t test).
doi:10.1371/journal.pone.0092904.g004

Absorptive enterocytes have a short life span (~5 days), being released into the gut lumen after they have migrated to the tip of villi. This elimination of IECs is thought to be triggered, at least in part, by spontaneous apoptosis [3]. To investigate whether the marked reduction in the numbers of absorptive enterocytes and goblet cells apparent in the intestine of Shp2 CKO mice might be attributable to an increased frequency of apoptosis, we performed immunostaining with antibodies to the cleaved form of caspase-3. However, the number of cleaved caspase-3–positive IECs in the ileum or colon of Shp2 CKO mice did not differ significantly from that for control mice (**Fig. S2**).

Impaired development of intestinal organoids from Shp2 CKO mice

The effect of Shp2 ablation in IECs on the development of villus structure from isolated crypts was investigated with the use of intestinal crypt-villus organoids [5]. The development of intestinal organoids from Shp2 CKO mice was found to be markedly impaired compared with that for control mice (**Fig. 6**). One day after seeding of isolated crypts, the morphology of the cultured crypts from Shp2 CKO mice was indistinguishable from that for control mice. However, 7 days after seeding, most of the crypts isolated from Shp2 CKO mice had failed to develop into intestinal

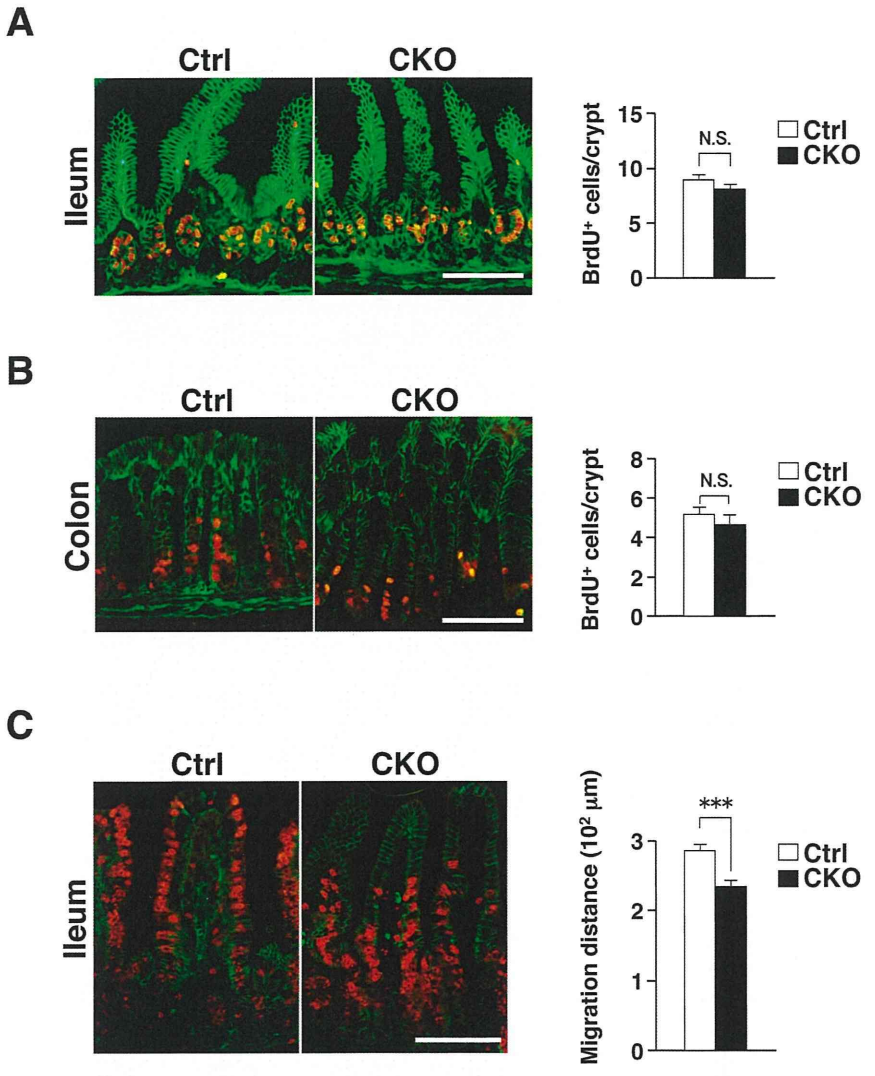

Figure 5. Impaired migration of IECs along the crypt-villus axis in the ileum of Shp2 CKO mice. A: Frozen sections of the ileum from 3- to 4-week-old control or Shp2 CKO mice at 2 h after BrdU injection were immunostained with mAbs to BrdU (red) and to β-catenin (green). Representative images are shown in the left panel. The number of BrdU-positive cells per crypt was determined (right panel). Data are means ± SE for 54 (control) or 77 (Shp2 CKO) crypts from a total of three (control) or four (Shp2 CKO) mice per group. N.S., not significant (Student's *t* test). **B**: Frozen sections of the colon from 3- to 4-week-old control or Shp2 CKO mice at 2 h after BrdU injection were immunostained as in **A**. The number of BrdU-positive cells per crypt was determined. Quantitative data are means ± SE for 54 (control) or 47 (Shp2 CKO) crypts from a total of three mice per group. N.S., not significant (Wilcoxon rank-sum test). **C**: Frozen sections of the ileum from 3- to 4-week-old control or Shp2 CKO mice at 2 days after BrdU injection were immunostained as in **A**. The distance from the crypt base to the farthest migrated BrdU-positive cells was measured. Quantitative data are means ± SE for 40 (control) or 48 (Shp2 CKO) villi from a total of three mice per group. ***$P<0.0001$ (Student's *t* test). All scale bars are 100 μm.
doi:10.1371/journal.pone.0092904.g005

organoids; they instead shrank or became cell debris. Quantitative analysis revealed that, whereas 66.6±9.9% of crypts from control mice developed into intestinal organoids, only 21.1±6.2% of those from Shp2 CKO mice did so. These results thus suggested that Shp2 is essential for efficient formation of intestinal organoids from isolated crypts.

Expression of activated K-Ras in IECs protects Shp2 CKO mice against colitis

Ras is an essential component of the signaling pathway by which growth factors stimulate cell proliferation, and the PTP activity of Shp2 is thought to regulate an upstream element necessary for Ras activation [10,11]. The phenotypes of Shp2 CKO mice were thus likely to be attributable at least in part to impairment of the activation of Ras in IECs. To examine this notion, we crossed Shp2 CKO mice with *LSL-Kras G12D* mice [17], which harbor a gene for an activated form of K-Ras (K-Ras^{G12D}). The crossing of Shp2 CKO (*Ptpn11*$^{fl/fl}$;villin-*cre*) mice with *LSL-Kras G12D* mice results in removal of translational stop elements by Cre-mediated recombination and consequent expression of the K-Ras^{G12D} gene under the control of its endogenous regulatory elements in an IEC-specific manner. Shp2 CKO;*LSL-Kras G12D* mice were born apparently healthy and phenotypically indistinguishable from their Shp2 CKO littermates (data not shown). Whereas Shp2 CKO mice were already sick at 4 weeks of age (**Fig. 2**), Shp2 CKO;*LSL-Kras G12D* mice (male or female) remained apparently healthy. Indeed, the body weight of Shp2 CKO;*LSL-Kras G12D* mice at 4 weeks of age was markedly greater

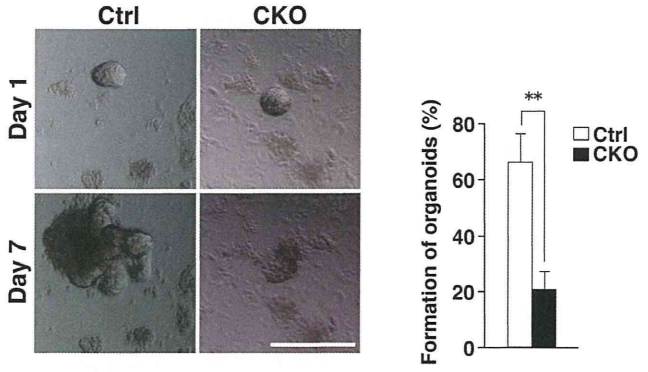

Figure 6. Impaired development of intestinal organoids from Shp2 CKO mice. Representative images of intestinal organoids derived from the jejunum of control or Shp2 CKO mice at 1 and 7 days after plating are shown in the left panel. Scale bar, 100 μm. The number of intestinal organoids with a crypt-villus structure at 7 days after plating was determined as a percentage of those with a spherelike morphology (diameter of >30 μm) at 1 day (right panel). Data are means ± SE for a total of 151 (control) or 128 (Shp2 CKO) organoids in four independent experiments. $^{**}P<0.01$ (Student's *t* test).
doi:10.1371/journal.pone.0092904.g006

than that of their Shp2 CKO littermates (**Table 1**), being similar to that of control mice (**Fig. 2A**). In addition, none of the Shp2 CKO;*LSL-Kras G12D* mice examined manifested any sign of colitis at or had died by 4.5 weeks of age (**Table 1**). Consistent with these findings, histological analysis of the ileum or colon from Shp2 CKO;*LSL-Kras G12D* mice revealed no sign of inflammation (**Fig. 7A**). These results thus suggested that expression of an active form of K-Ras in IECs protected Shp2 CKO mice from the development of colitis. We also found that the number of β-catenin –positive absorptive enterocytes was increased and that of Paneth cells was reduced in the ileum of Shp2 CKO;*LSL-Kras G12D* mice compared with those for Shp2 CKO mice at 4.5 weeks of age (**Fig. 7B**). In addition, we found that the number of mucin 2–positive goblet cells in the ileum or colon of Shp2 CKO;*LSL-Kras G12D* mice at 4.5 weeks of age was markedly greater than that for Shp2 CKO mice (**Fig. 7C**). The number of mucin 2–positive goblet cells in the ileum of Shp2 CKO;*LSL-Kras G12D* mice (22±1 per villus) was similar to or even slightly greater than that apparent in control mice (18 1 per villus) (**Fig. 4B**). Together, these findings suggested that crossing of Shp2 CKO mice with *LSL-Kras G12D* mice restores the phenotypes of the former animals to normal.

Discussion

We have here shown that mice lacking Shp2 specifically in IECs develop severe colitis. The numbers of absorptive enterocytes and goblet cells were markedly reduced in the small intestine and colon of the mutant mice compared with those for control animals. Moreover, the development of intestinal organoids from isolated crypts of the Shp2 CKO mice was impaired. Shp2 is thought to be indispensable for activation of the Ras-MAPK signaling pathway and thereby for the promotion of cell proliferation and differentiation [10,11,25]. Shp2 in the nucleus is also important for activation of Wnt signaling [26], which is a key regulator of the proliferation and differentiation of IECs [2]. However, the colitis as well as the reduction in the number of absorptive enterocytes and goblet cells in the ileum of Shp2 CKO mice were prevented by expression of an activated form of K-Ras in IECs. Our present results thus indicate that Shp2 in IECs is important for protection against colitis as well as for homeostatic regulation of absorptive enterocytes and goblet cells, and that these functions of Shp2 are mediated through activation of the Ras-MAPK signaling pathway. The development of intestinal organoids essentially requires epidermal growth factor, which promotes IEC growth by activation of Ras-MAPK signalling, in the culture medium [5]. Thus, the impaired development of organoids from isolated crypts of the Shp2 CKO mice is most likely attributable to the impaired effect of epidermal growth factor on organoid development. Moreover, such impaired development of organoids in the culture system is well consistent with the IEC phenotype of Shp2 CKO mice such as reduced numbers of absorptive enterocytes and goblet cells, two major cell populations in IECs.

Shp2 is indispensable for embryogenesis at the early stages of gastrulation and mesoderm patterning [14]. In addition, conditional ablation of Shp2 in hematopoietic stem cells induces bone marrow aplasia [27], suggesting that Shp2 is essential for hematopoiesis from stem cells in the bone marrow. Given that Cre recombinase is expressed throughout the presumptive intestine of *villin-cre* mice by 14.5 days post coitum [18], ablation of Shp2 in the embryonic intestinal epithelium likely occurs in our Shp2 CKO mice. It is therefore of note that Shp2 CKO mice were born apparently healthy and that the overall development and morphology of the intestinal epithelium in these animals appeared almost normal up to 2 to 3 weeks of age (data not shown). Indeed, the population of Olfm4 mRNA–positive stem cells and BrdU incorporation into TA cells in crypts were not significantly affected in the small intestine of Shp2 CKO mice compared with control mice. Unlike the hematopoietic cell system, the Shp2-Ras signaling pathway thus does not appear to play a key role in the homeostasis of stem cells or in TA cell proliferation in the intestinal epithelium. In contrast, the Wnt signaling pathway is thought to be required for maintenance of intestinal stem cells as well as for the proliferation of IECs generated from these stem cells [2]. Indeed, ablation of the transcription factor Tcf-4, which is essential for operation of the Wnt signaling pathway in IECs, was found to result in marked defects in the development of intestinal villi, including the complete absence of the intestinal progenitor compartment [28].

Our results indicate that the Shp2-Ras signaling pathway is important for the development of mature IECs, in particular for that of absorptive enterocytes and goblet cells. The number of absorptive enterocytes in the small intestine was markedly reduced in Shp2 CKO mice. In addition, the number of goblet cells was also reduced in both the small intestine and colon of Shp2 CKO mice. Consistent with this finding, activation of K-Ras in IECs was previously shown to result in hyperplasia of the intestinal epithelium (suggesting an increase of absorptive enterocytes) as well as a marked increase in the number of goblet cells [29,30]. Indeed, the reduction in the numbers of absorptive enterocytes and goblet cells in the ileum of Shp2 CKO mice was prevented by expression of an activated form of K-Ras in IECs. Thus, the Shp2-Ras signaling pathway is indeed important for the development of absorptive enterocytes and goblet cells. In contrast, Shp2 CKO mice manifested a significant increase in the number of Paneth cells in crypts. Conversely, we also showed that such increased number of Paneth cells was prevented by expression of an activated form of K-Ras in IECs. It was also showed that activation of K-Ras in IECs resulted in a marked reduction in the number of Paneth cells [30]. Thus, the Shp2-Ras signaling likely participates in negative regulation of the Paneth cell population.

The etiology of colitis in Shp2 CKO mice remains to be fully characterized. Goblet cells in the intestinal epithelium are thought to form a mucosal barrier by secreting mucus and thereby to protect against the development of intestinal inflammation [31].

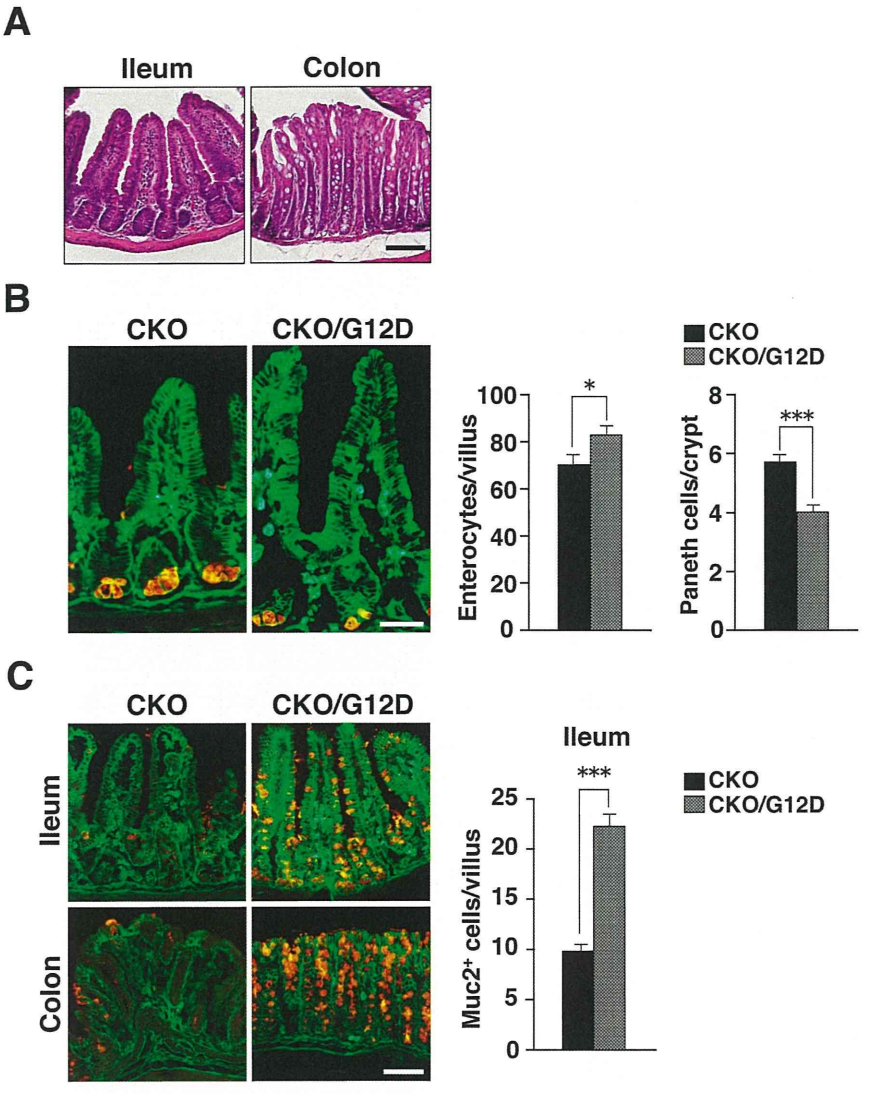

Figure 7. Expression of activated K-Ras in IECs protects Shp2 CKO mice against colitis. A: Hematoxylin-eosin staining of the ileum and colon from Shp2 CKO;*LSL-Kras G12D* mice at 4.5 weeks of age. Images are representative of those from three mice. Scale bar, 100 μm. **B**: Frozen sections of the ileum and colon from Shp2 CKO;*LSL-Kras G12D* (CKO/G12D) mice and their Shp2 CKO littermates at 4.5 weeks of age were immunostained with antibodies to lysozyme (red) and to β-catenin (green). Representative images are shown in the left panel. Scale bar, 100 μm. The middle panel shows the number of β-catenin –positive absorptive enterocytes per villus of the ileum. Data are means ± SE for 14 (CKO/G12D) or 10 (CKO) villi from a total of three (CKO/G12D) or two (CKO) mice per group. *$P<0.05$ (Student's *t* test). The right panel shows lysozyme-positive Paneth cells per crypt of the ileum. Data are means ± SE for 60 (CKO/G12D) or 43 (CKO) crypts from a total of three (CKO/G12D) or two (CKO) mice per group. ***$P<0.0001$ (Student's *t* test). **C**: Frozen sections of the ileum and colon from Shp2 CKO;*LSL-Kras G12D* (CKO/G12D) mice and their Shp2 CKO littermates at 4.5 weeks of age were immunostained with antibodies to mucin 2 (red) and to β-catenin (green). Representative images are shown in the left panel. Scale bar, 100 μm. The number of mucin 2–positive goblet cells per villus of the ileum was determined (right panel). Data are means ± SE for 30 (CKO/G12D) or 21 (CKO) villi from a total of three (CKO/G12D) or two (CKO) mice per group. ***$P<0.0001$ (Welch's *t* test).
doi:10.1371/journal.pone.0092904.g007

Table 1. Phenotypes of three Shp2 CKO;*LSL-Kras G12D* mice and three Shp2 CKO littermates at 4.5 weeks of age.

Genotype	Sex	Body weight (g)	Disease activity index
CKO	Male	5.8	Dead
CKO	Male	7.5	6
CKO	Female	7.6	2
CKO/*Kras G12D*	Male	9.2	0
CKO/*Kras G12D*	Female	10.3	0
CKO/*Kras G12D*	Female	11.8	0

doi:10.1371/journal.pone.0092904.t001

Mucin 2 is the most abundant mucin produced by goblet cells, and deletion or mutation of the mucin 2 gene in mice results in the spontaneous development of colitis [32,33]. The development of intestinal inflammation in Shp2 CKO mice is therefore most likely attributable to the marked reduction in the number of goblet cells in the intestine. Absorptive enterocytes are most abundant IECs and they form a physiological barrier against the intestinal microflora. We showed that the number of absorptive enterocytes was markedly reduced in Shp2 CKO mice, suggesting that the impairment of the physiological barrier provided by the intestinal epithelium likely occurs in Shp2 CKO mice. During the course of the present study, Coulombe et al. also showed that ablation of Shp2 in IECs resulted in the spontaneous development of colitis [34]. They also showed that expression of tight junctional proteins such as claudin was markedly reduced in the colon of their mutant mice, resulting in an increase in intestinal permeability [34]. Collectively, a defect in the physical barrier provided by the intestinal epithelium is likely a contributing factor to the development of colitis in Shp2 CKO mice. The number of Paneth cells was slightly increased in the ileum of Shp2 CKO mice. Paneth cells produce antimicrobial peptide such as α- or β-defensin, which are thought to be important for preventing the growth of pathogenic microbes [35,36]. Thus, the increase of Paneth cells unlikely participates in the development of colitis in Shp2 CKO mice. The prevention of epithelial cell death by conditional ablation of caspase-8 in mouse IECs was also found to induce intestinal inflammation [37], suggesting that proper turnover of these cells is also important for homeostasis of intestinal immunity. In the present study, we found that IEC-specific ablation of Shp2 resulted in impaired migration of IECs along the crypt-villus axis. A delayed turnover of IECs may thus also contribute to intestinal inflammation in Shp2 CKO mice.

In summary, we have shown that Shp2 is necessary for homeostasis of IECs, in particular for that of absorptive enterocytes and goblet cells, as well as for protection against colitis. These functions of Shp2 are likely mediated by activation of Ras. Further investigation will be required, however, to clarify the molecular mechanism by which Shp2 in IECs regulates intestinal immunity and protects against colitis.

Supporting Information

Figure S1 Specific expression of β-galactosidase in the ileum and colon of R26R;villin-cre mice. Frozen sections of the ileum or colon from adult *R26R*;villin-*cre* mice were stained for β-galactosidase activity (blue). Scale bar, 100 μm.
(TIFF)

Figure S2 Lack of effect of Shp2 ablation on the number of apoptotic IECs in the ileum or colon. Frozen sections of the ileum (**A**) or colon (**B**) from control or Shp2 CKO mice at 3 weeks of age were immunostained with antibodies to cleaved caspase-3 (red) and to β-catenin (green). Representative images are shown in the left panels. Scale bars, 100 μm. The number of cleaved caspase-3–positive cells per 10 villi in the ileum or 10 intestinal glands in the colon was determined (right panels). Data are means ± SE for 104 (control) or 118 (Shp2 KO) villi of the ileum and for 95 (control) or 92 (Shp2 CKO) intestinal glands of the colon from a total of two mice per group. N.S., not significant (Wilcoxon rank-sum test).
(TIFF)

Acknowledgments

We thank T. Sato (Keio University) for technical support, B. G. Neel (Princess Margaret Cancer Centre) for providing *Ptpn11*$^{fl/fl}$ mice, C. J. Kuo (Stanford University) for providing HEK293T cells expressing R-spondin1–Fc, as well as M. Tei and M. Inagaki for technical assistance.

Author Contributions

Conceived and designed the experiments: TM H. Okazawa YM. Performed the experiments: HY TK JP. Analyzed the data: HY TK JP. Contributed reagents/materials/analysis tools: H. Ohnishi YK. Wrote the paper: TM TK.

References

1. Blanpain C, Horsley V, Fuchs E (2007) Epithelial stem cells: turning over new leaves. Cell 128: 445–458.
2. van der Flier LG, Clevers H (2009) Stem cells, self-renewal, and differentiation in the intestinal epithelium. Annu Rev Physiol 71: 241–260.
3. Hall PA, Coates PJ, Ansari B, Hopwood D (1994) Regulation of cell number in the mammalian gastrointestinal tract: the importance of apoptosis. J Cell Sci 107 (Pt 12): 3569–3577.
4. Eisenhoffer GT, Loftus PD, Yoshigi M, Otsuna H, Chien CB, et al. (2012) Crowding induces live cell extrusion to maintain homeostatic cell numbers in epithelia. Nature 484: 546–549.
5. Sato T, Vries RG, Snippert HJ, van de Wetering M, Barker N, et al. (2009) Single Lgr5 stem cells build crypt-villus structures in vitro without a mesenchymal niche. Nature 459: 262–265.
6. Holmberg J, Genander M, Halford MM, Anneren C, Sondell M, et al. (2006) EphB receptors coordinate migration and proliferation in the intestinal stem cell niche. Cell 125: 1151–1163.
7. Batlle E, Henderson JT, Beghtel H, van den Born MM, Sancho E, et al. (2002) Beta-catenin and TCF mediate cell positioning in the intestinal epithelium by controlling the expression of EphB/ephrinB. Cell 111: 251–263.
8. Sadakata H, Okazawa H, Sato T, Supriatna Y, Ohnishi H, et al. (2009) SAP-1 is a microvillus-specific protein tyrosine phosphatase that modulates intestinal tumorigenesis. Genes Cells 14: 295–308.
9. Noguchi T, Tsuda M, Takeda H, Takada T, Inagaki K, et al. (2001) Inhibition of cell growth and spreading by stomach cancer-associated protein-tyrosine phosphatase-1 (SAP-1) through dephosphorylation of p130cas. J Biol Chem 276: 15216–15224.
10. Matozaki T, Murata Y, Saito Y, Okazawa H, Ohnishi H (2009) Protein tyrosine phosphatase SHP-2: a proto-oncogene product that promotes Ras activation. Cancer Sci 100: 1786–1793.
11. Neel BG, Gu H, Pao L (2003) The 'Shp'ing news: SH2 domain-containing tyrosine phosphatases in cell signaling. Trends Biochem Sci 28: 284–293.
12. Kodama A, Matozaki T, Fukuhara A, Kikyo M, Ichihashi M, et al. (2000) Involvement of an SHP-2-Rho small G protein pathway in hepatocyte growth factor/scatter factor-induced cell scattering. Mol Biol Cell 11: 2565–2575.
13. Schoenwaelder SM, Petch LA, Williamson D, Shen R, Feng GS, et al. (2000) The protein tyrosine phosphatase Shp-2 regulates RhoA activity. Curr Biol 10: 1523–1526.
14. Saxton TM, Henkemeyer M, Gasca S, Shen R, Rossi DJ, et al. (1997) Abnormal mesoderm patterning in mouse embryos mutant for the SH2 tyrosine phosphatase Shp-2. EMBO J 16: 2352–2364.
15. Fornaro M, Burch PM, Yang W, Zhang L, Hamilton CE, et al. (2006) SHP-2 activates signaling of the nuclear factor of activated T cells to promote skeletal muscle growth. J Cell Biol 175: 87–97.
16. Soriano P (1999) Generalized lacZ expression with the ROSA26 Cre reporter strain. Nat Genet 21: 70–71.
17. Jackson EL, Willis N, Mercer K, Bronson RT, Crowley D, et al. (2001) Analysis of lung tumor initiation and progression using conditional expression of oncogenic K-ras. Genes Dev 15: 3243–3248.
18. Madison BB, Dunbar L, Qjao XT, Braunstein K, Braunstein E, et al. (2002) Cis elements of the villin gene control expression in restricted domains of the vertical (crypt) and horizontal (duodenum, cecum) axes of the intestine. J Biol Chem 277: 33275–33283.
19. Murata Y, Mori M, Kotani T, Supriatna Y, Okazawa H, et al. (2010) Tyrosine phosphorylation of R3 subtype receptor-type protein tyrosine phosphatases and their complex formations with Grb2 or Fyn. Genes Cells 15: 513–524.
20. Siegmund B, Sennello JA, Lehr HA, Batra A, Fedke I, et al. (2004) Development of intestinal inflammation in double IL-10- and leptin-deficient mice. J Leukoc Biol 76: 782–786.
21. Kanazawa Y, Saito Y, Supriatna Y, Tezuka H, Kotani T, et al. (2010) Role of SIRPα in regulation of mucosal immunity in the intestine. Genes Cells 15: 1189–1200.
22. Barker N, Clevers H (2010) Lineage tracing in the intestinal epithelium. Curr Protoc Stem Cell Biol Chapter 5: Unit5A 4.

23. van Es JH, Sato T, van de Wetering M, Lyubimova A, Nee AN, et al. (2012) Dll1^{+} secretory progenitor cells revert to stem cells upon crypt damage. Nat Cell Biol 14: 1099–1104.
24. van der Flier LG, Haegebarth A, Stange DE, van de Wetering M, Clevers H (2009) OLFM4 is a robust marker for stem cells in human intestine and marks a subset of colorectal cancer cells. Gastroenterology 137: 15–17.
25. Noguchi T, Matozaki T, Horita K, Fujioka Y, Kasuga M (1994) Role of SH-PTP2, a protein-tyrosine phosphatase with Src homology 2 domains, in insulin-stimulated Ras activation. Mol Cell Biol 14: 6674–6682.
26. Takahashi A, Tsutsumi R, Kikuchi I, Obuse C, Saito Y, et al. (2011) SHP2 tyrosine phosphatase converts parafibromin/Cdc73 from a tumor suppressor to an oncogenic driver. Mol Cell 43: 45–56.
27. Grossmann KS, Wende H, Paul FE, Cheret C, Garratt AN, et al. (2009) The tyrosine phosphatase Shp2 (PTPN11) directs Neuregulin-1/ErbB signaling throughout Schwann cell development. Proc Natl Acad Sci U S A 106: 16704–16709.
28. Korinek V, Barker N, Willert K, Molenaar M, Roose J, et al. (1998) Two members of the Tcf family implicated in Wnt/beta-catenin signaling during embryogenesis in the mouse. Mol Cell Biol 18: 1248–1256.
29. Haigis KM, Kendall KR, Wang Y, Cheung A, Haigis MC, et al. (2008) Differential effects of oncogenic K-Ras and N-Ras on proliferation, differentiation and tumor progression in the colon. Nat Genet 40: 600–608.
30. Feng Y, Bommer GT, Zhao J, Green M, Sands E, et al. (2011) Mutant KRAS promotes hyperplasia and alters differentiation in the colon epithelium but does not expand the presumptive stem cell pool. Gastroenterology 141: 1003–1013 e1001–1010.
31. McGuckin MA, Linden SK, Sutton P, Florin TH (2011) Mucin dynamics and enteric pathogens. Nat Rev Microbiol 9: 265–278.
32. Van der Sluis M, De Koning BA, De Bruijn AC, Velcich A, Meijerink JP, et al. (2006) Muc2-deficient mice spontaneously develop colitis, indicating that MUC2 is critical for colonic protection. Gastroenterology 131: 117–129.
33. Heazlewood CK, Cook MC, Eri R, Price GR, Tauro SB, et al. (2008) Aberrant mucin assembly in mice causes endoplasmic reticulum stress and spontaneous inflammation resembling ulcerative colitis. PLoS Med 5: e54.
34. Coulombe G, Leblanc C, Cagnol S, Maloum F, Lemieux E, et al. (2013) Epithelial tyrosine phosphatase SHP-2 protects against intestinal inflammation in mice. Mol Cell Biol 33: 2275–2284.
35. Ouellette AJ (2005) Paneth cell alpha-defensins: peptide mediators of innate immunity in the small intestine. Springer Semin Immunopathol 27: 133–146.
36. Shi J (2007) Defensins and Paneth cells in inflammatory bowel disease. Inflamm Bowel Dis 13: 1284–1292.
37. Gunther C, Martini E, Wittkopf N, Amann K, Weigmann B, et al. (2011) Caspase-8 regulates TNF-α-induced epithelial necroptosis and terminal ileitis. Nature 477: 335–339.

Virology 462-463 (2014) 166–174

Contents lists available at ScienceDirect

Virology

journal homepage: www.elsevier.com/locate/yviro

Rab18 is required for viral assembly of hepatitis C virus through trafficking of the core protein to lipid droplets

Hiromichi Dansako [a], Hiroki Hiramoto [a], Masanori Ikeda [a], Takaji Wakita [b], Nobuyuki Kato [a,*]

[a] Department of Tumor Virology, Okayama University Graduate School of Medicine, Dentistry and Pharmaceutical Sciences, 2-5-1 Shikata-cho, Kita-ku, Okayama 700-8558, Japan
[b] Department of Virology II, National Institute of Infectious Disease, 1-23-1 Toyama, Shinjuku-ku, Tokyo 162-8640, Japan

ARTICLE INFO

Article history:
Received 14 February 2014
Returned to author for revisions
11 March 2014
Accepted 14 May 2014

Keywords:
Hepatitis C virus
Rab18
Viral assembly
Lipid droplet
Core protein
RNA replication

ABSTRACT

During persistent infection of HCV, the HCV core protein (HCV-JFH-1 strain of genotype 2a) is recruited to lipid droplets (LDs) for viral assembly, but the mechanism of recruitment of the HCV core protein is uncertain. Here, we demonstrated that one of the Ras-related small GTPases, Rab18, was required for trafficking of the core protein around LDs. The knockdown of Rab18 reduced intracellular and extracellular viral infectivity, but not intracellular viral replication in HCV-JFH-1-infected RSc cells (an HuH-7-derived cell line). Exogenous expression of Rab18 increased extracellular viral infectivity almost two-fold. Furthermore, Rab18 was co-localized with the core protein in HCV-JFH-1-infected RSc cells, and the knockdown of Rab18 blocked recruitment of the HCV-JFH-1 core protein to LDs. These results suggest that Rab18 has an important role in viral assembly through the trafficking of the core protein to LDs.

Introduction

Hepatitis C virus (HCV) is an enveloped positive single-stranded RNA virus belonging to the *Flaviviridae* family (Choo et al., 1989). The HCV genome encodes a large polyprotein precursor of approximately 3000 amino acid (aa) residues, which is cleaved co- and post-translationally into at least ten proteins in the following order: core, envelope 1 (E1), E2, p7, nonstructural protein 2 (NS2), NS3, NS4A, NS4B, NS5A, and NS5B (Kato, 2001). Persistent HCV infection in the liver causes chronic hepatitis, and then highly progresses to liver cirrhosis and hepatocellular carcinoma (Ohkoshi et al., 1990). Therefore, the elimination of HCV RNA by the anti-HCV reagents such as interferon is necessary to block the progression of liver diseases such as liver cirrhosis and hepatocellular carcinoma. To date, the HCV-JFH-1 strain (genotype 2a) has mainly been used to study the complete life cycle of HCV worldwide. In HCV-JFH-1-infected human hepatoma HuH-7 cells, viral replication intermediate, double-stranded RNA, is detected adjacent to the membranes of the endoplasmic reticulum (ER) (Targett-Adams et al., 2008). In addition, the HCV replication complex is formed on a detergent-resistant membrane (Shi et al., 2003). These results suggest that HCV RNA replication occurs on lipid rafts and the membranous web at the cytosolic side of the ER. Following viral replication, the HCV core protein matures through the translation of a large polyprotein precursor from HCV RNA and then the processing by signal peptide peptidase. The matured HCV-JFH-1 core protein has been shown to be trafficked to lipid droplets (LDs) for viral assembly (Miyanari et al., 2007).

LDs are important organelles for lipid metabolism. LDs are covered by a phospholipid monolayer, and accumulate excessive neutral lipids such as triglycerides. A proteomics analysis revealed that a number of host factors are associated with LDs (Brasaemle et al., 2004). These host factors are required for acquisition, storage, lipolysis, transport and/or release of lipids, respectively. The first of these LD-associated factors to be identified were members of the PAT family of proteins, including perilipin (PLIN), ADRP (adipose differentiation-related protein; also named adipophilin or PLIN2), and TIP47 (also named PLIN3). PLIN is expressed only in adipocytes and steroidogenic cells, whereas ADRP and TIP47 are expressed in various cell types. ADRP and TIP47 have similar sequences and three-dimensional structures (Hickenbottom et al., 2004), but their intracellular distributions in HuH-7 cells are different (Ohsaki et al., 2006). ADRP localizes exclusively to the surface of LDs in HuH-7 cells, whereas only some of total TIP47 localizes to the LD surface in this cell line. During viral assembly, the core protein is trafficked to ADRP on LDs (Counihan et al., 2011). ADRP is displaced from the surface of LDs to the cytoplasm by the core protein, and then subjected to degradation (Boulant et al., 2008). These displacements

* Corresponding author. Fax: +81 86 235 7392.
E-mail address: nkato@md.okayama-u.ac.jp (N. Kato).

http://dx.doi.org/10.1016/j.virol.2014.05.017
0042-6822/

of ADRP also cause the redistribution of LDs around the nucleus (Boulant et al., 2008). These observations imply that the core protein may increase the probability of an interaction between the sites of viral replication at the ER and viral assembly at the LDs. However, the precise mechanism of intracellular trafficking of the core protein to ADRP on LDs is still uncertain.

A family of Ras-related small GTPases plays an important role in the membrane trafficking between organelles such as the ER, Golgi, early/late endosomes, LDs, and so on (Hutagalung and Novick, 2011). One of the Ras-related small GTPases, Rab18, is required for membrane trafficking between the ER and Golgi (Dejgaard et al., 2008). On the other hand, Rab18 is an LD-associated protein, and the ectopic expression of Rab18 induces the close apposition of LDs to ER membranes through the reduction of ADRP (Ozeki et al., 2005). These observations imply that Rab18 may be required for membrane trafficking through the redistribution of LDs around the ER. Recently, Salloum et al. reported that Rab18 bound HCV-JFH-1 NS5A and may have promoted the interaction between sites of viral replication and LDs in HCV-Jc1-infected Huh7.5.1 cells (Salloum et al., 2013). However, HCV-Jc1 is an intragenotypic recombinant encoding core to NS2 from the HCV-J6 strain (genotype 2a) in the context of HCV-JFH-1, and does not exist in nature. In addition, although HCV-Jc1 was shown to be more robust in the release of viral particles than HCV-JFH-1, the HCV-J6 core protein did not associate with LDs (Shavinskaya et al., 2007). On the other hand, the HCV-JFH-1 core protein does associate with LDs, and LD-associated core proteins recruit HCV NS protein from the ER to LDs (Miyanari et al., 2007). These results imply that HCV-Jc1 may release viral particles via an intracellular organelle distinct from the LDs. Therefore, we hypothesized that Rab18 first trafficked the HCV-JFH-1 core protein and subsequently NS5A to LD. To prove this hypothesis, we examined the association of the HCV-JFH-1 core protein with LDs and the levels of viral assembly in Rab18-knockdown cells.

Here, we show that Rab18 is required for trafficking of the HCV-JFH-1 core protein to LDs and the subsequent assembly of HCV. Rab18 may be involved in the maturation of viral particles through membrane trafficking of the HCV-JFH-1 core protein from the sites of viral replication at the ER to viral assembly at the LDs in human hepatocytes.

Results

RSc cells show higher viral productivity than Huh7.5 cells

To date, human hepatoma HuH-7 cells have mainly been used to study the complete life cycle of HCV in studies worldwide. One of the sublines of HuH-7 cells, Huh7.5, is used in many laboratories for its high susceptibility to infection with the HCV-JFH-1 strain (genotype 2a). On the other hand, we have previously established several types of HCV RNA-replicating cells (genotype 1b, O strain), such as sO cells (Kato et al., 2003, sub-genomic HCV RNA), O cells (Ikeda et al., 2005, genome-length HCV RNA), and OR6 cells (Ikeda et al., 2006, genome-length HCV RNA-encoding renilla luciferase) derived from HuH-7 cells, and their "cured" cells (sOc (Kato et al., 2003), Oc (Ikeda et al., 2005), OR6c (Ikeda et al., 2006), respectively) by the elimination of HCV RNA (Fig. 1A). The cured cell lines have been reported to increase the permissiveness of HCV (Blight et al., 2002). We also previously reported that Oc cells showed higher permissiveness of HCV than sOc cells (Abe et al., 2007). RSc cells are one of our cured cell lines derive from OR6c cells, and have mainly been used to study the complete life cycle of HCV in our laboratory (Ariumi et al., 2007, 2008; Kato et al., 2009). However, we have no information on viral susceptibility of our cured cell lines to HCV-JFH-1 infection. To identify which of our cured cell lines would be most useful for the infection with HCV-JFH-1, we first compared the amounts of LDs by two methods, i.e., a confocal microscope and flow cytometry. The LDs were stained with BODIPY493/503 and observed under a confocal microscope. In our cured cells (sOc, Oc, OR6c, and RSc cells), the numbers rather than the sizes of LDs have increased compared to HuH-7 cells (Fig. 1B). In addition, the mean fluorescence intensity of BODIPY493/503-stained cells has increased by the enhancements of the numbers of LDs (Fig. 1C). These qualitative and quantitative analyses revealed that our cured cells (sOc, Oc, OR6c, and RSc cells) formed higher levels of LDs than HuH-7 and Huh7.5 cells (Fig. 1B and C). Interestingly, irrespective of the quantitative difference of LDs, the levels of viral replication at 72 h after the viral inoculation of HCV-JFH-1 were comparable between each of our cured cell lines and Huh7.5 cells, but not between each of the cured cell lines and HuH-7 cells (Fig. 1D). Moreover, the time-course analysis showed that the capacities of HCV RNA replication were almost comparable between RSc and Huh7.5 cells (Fig. 1E). These results suggest that the levels of HCV RNA replication do not depend on the amount of LDs. Next, to compare the levels of viral assembly and viral productivity between RSc and Huh7.5 cells, we examined the infectivity of the cell lysates (intracellular infectivity) and the supernatants (extracellular infectivity) derived from both lines of HCV-JFH-1-infected cells. The intracellular and extracellular infectivities of HCV-JFH-1-infected RSc cells were significantly higher than those of HCV-JFH-1-infected Huh7.5 cells (Fig. 1F). These results suggest that RSc cells possess higher viral productivity in response to infection with HCV-JFH-1 than Huh7.5 cells.

Rab18 is required for viral production, but not viral RNA replication

As the first step of viral assembly, the HCV-JFH-1 core protein displaces ADRP from the surface of LDs to the cytoplasm (Boulant et al., 2008; Counihan et al., 2011). In the present study, we tried to clarify how the core protein is trafficked to LDs by using RSc and Huh7.5 cells. It has been reported that Rab18, one of the Ras-related small GTPase family members, induces the close apposition of LDs to ER membranes through the reduction of ADRP (Ozeki et al., 2005). Based on these previous findings, we hypothesized that Rab18 is required for trafficking of the HCV-JFH-1 core protein to LDs. To prove this hypothesis, we first examined the expression levels of Rab18 in RSc and Huh7.5 cells. The expression levels of Rab18 were almost comparable between RSc cells and Huh7.5 cells at both the transcript (Fig. 2A) and protein levels (Fig. 2B). Two other members of the Ras-related small GTPases, Rab5 and Rab7, were also present at almost the same levels in RSc and Huh7.5 cells. We next examined the effect of the knockdown of Rab18 against HCV replication in RSc cells. The knockdown of Rab18 (Fig. 2C) had no effect on the RNA replication step (Fig. 2D). Rab18-knockdown Huh7.5 cells and genome-length HCV RNA-replicating O cells (Kato et al., 2009) also showed similar results (Fig. 2E and F, Supplemental Fig. S1A and B). However, we found that the knockdown of Rab18 caused a significant decrease in viral productivity in both RSc and Huh7.5 cells (Fig. 2G). In addition, the knockdown of ADRP (Supplemental Fig. S2A) also decreased viral productivity rather than HCV RNA replication (Supplemental Fig. S2B). Furthermore, we demonstrated that the overexpression of Rab18 (Fig. 2H) recovered the viral productivity (Fig. 2I) rather than viral RNA replication (Fig. 2J). From these results, we conclude that Rab18 is required for viral production of HCV.

Rab18 is required for viral assembly through the trafficking of the HCV-JFH-1 core protein to LDs

To clarify whether Rab18 is required for the viral assembly step, we first examined the localization of Rab18 and the HCV core protein in HCV-JFH-1-infected cells. The results revealed that Rab18